AUIQ Technical Engineering Science

Manuscript 1023

Surface Urban Heat Island Effects Analysis in the Most Populated City in Thailand: Towards Sustainable Urban Development

Abdul Maulud Khairul Nizam

Muhammad Noor

Zafar Iqbal

AUIQ TECHNICAL ENGINEERING SCIENCE 2025;2:33–53

ORIGINAL STUDY

Surface Urban Heat Island Effects Analysis in the Most Populated City in Thailand: Towards Sustainable Urban Development

Abdul Maulud Khairul Nizam [a], Muhammad Noor [b], Zafar Iqbal [c,*]

[a] Department of Civil Engineering, Faculty of Engineering and Built Environment, Universiti Kebangsaan Malaysia, Bangi 43600 UKM, Selangor, Malaysia
[b] Balochistan University of Engineering and Technology, Khuzdar, Pakistan
[c] NUST Institute of Civil Engineering-SCEE, National University of Sciences and Technology (NUST), H-12, Islamabad, 44000, Pakistan

ABSTRACT

The fast and unprecedented urban growth process may violate cities' responsibilities by causing an urban heat island (UHI) and increasing the public's risk of heat-related illnesses due to vegetative area reduction and urban area inclination. The Bangkok Metropolitan Area (BMA)'s variations in Land Use Land Cover (LULC), Land Surface Temperature (LST), UHI, and several geospatial indicators, as well as the daytime and nighttime LST, are the main subjects of the study. Between 2015 and 2021, the highest Daytime LST (DLST) rose consistently from 36.77°C to 38.14°C, then slightly decreased to 37.22°C in 2023. There is a general increase in the maximum Surface Urban Heat Island (SUHI) intensity from 1.112 (2015) to 1.162 (2021), and then a minor decrease to 1.157 (2023). With the highest values circling 11.0 and the lowest around 7.32, UTFVI levels stayed reasonable between 2015 and 2018. Nonetheless, there has been a discernible increase in high-heat zones since 2019, with peak UTFVI values continuously exceeding 11.0 and rising to 12.19 by 2023. SAVI readings over the observed time vary from a low of roughly −0.088 to a high of 0.398. Consistent urban expansion is suggested by the significant increase in the maximum NDBI values over the nine years, especially from 2015 (0.057) to 2021 (0.081). To lower the risks and offer practical answers, the city planners and officials implement sustainable urban development and urban resilience by adopting sustainable urban design techniques, such as incorporating green infrastructure, preserving vegetation-rich regions, and putting heat-mitigation techniques like rooftop gardens, urban parks, and permeable surfaces into practice, is crucial to overcoming these obstacles.

Keywords: Heat island effects, Climate change, Urban resilience, Bangkok, Urban sustainability

1. Introduction

The physical environment of cities has altered as a result of urbanization, and these changes have happened quickly because of economic growth and population concentration [1]. The physical environment of cities has changed, and this has led to changes in the urban climate [2, 4]. These developments have also impacted the severity of urban climate change, as urbanization keeps growing cities and making their physical forms denser. More so than global climate change, urbanization-induced urban climate change has impacted metropolitan thermal conditions [5, 6]. Particularly in cities where extreme heat events have been exacerbated by urban climate change, urban heating is an issue. Numerous factors, such as the high thermal mass released by concrete and asphalt roads, the low ventilation capacity of urban canyons created by high-rise buildings, and the combined effect of heat released from vehicles on streets and air conditioners [7], all contribute to and amplify the rise in ambient temperature brought on by urban climate

Received 30 January 2025; revised 9 March 2025; accepted 25 March 2025.
Available online 30 April 2025

* Corresponding author.
E-mail addresses: knam@ukm.edu.my (A. M. Khairul Nizam), mnkakar@gmail.com (M. Noor), zafar.thalvi@nice.nust.edu.pk (Z. Iqbal).

https://doi.org/10.70645/3078-3437.1023

change [8, 10]. Based on certain numerical indicators specifically, an increase in air temperature in particular parts of cities the UHI is a picture of urban climate change [11]. The potent force of UHI strengthens heat waves, and vice versa [12]. The intensity of UHIs has been rising quickly in large cities over the past several years, which has resulted in higher energy consumption and serious health issues for city people [13]. The need for more thorough research and analysis to comprehend the decline of urban heat environments is growing as heat waves and UHIs in cities occur more frequently and with greater severity [9, 14].

There are numerous instances of high urban temperatures around the world, which result from the rapid urbanization process and the effects of global warming [15]. Samut Prakan, Pathum Thani, Samut Sakhon, Nakhon Pathom, and Nonthaburi are the five additional metropolitan provinces that makeup Thailand's main urban centers, together with the capital of Bangkok. These regions together cover a vast area of 7761.66 km^2 [16]. Known as the Metropolis, this area is the hub of the economy where various facilities, services, and activities come together. The Metropolis has experienced the interaction of agglomeration economies, which has led to the blending of social and economic components [17]. On the other hand, this phenomenon has caused traffic in the primate city and sparked a decentralized suburbanization movement [18]. At the same time, various innovations have been sparked by the fast pace of urbanization, extending metropolitan areas into neighbouring provinces. Alongside this growth, there have been increased investments in land transportation, with a focus on improving connectivity with the city center via highway and motorway networks rather than giving public transportation priority [19]. The UHIs are a result of the expansion of urban areas, which changes the link between surface albedo and the thermal properties of LULC conditions in urban contexts [20, 21]. A UHI is a condition where the temperature in a metropolitan area is much higher than the temperature in the surrounding areas. This is mostly caused by changes in land surfaces brought about by urban development. In Thailand, researchers examined Bangkok, the capital of Thailand, using the modified vegetation index to determine its UHI [22]. The LST in greater Bangkok, or the city's core business district, was up to 3.5 °C warmer than in peri-urban locations. Researchers found that using historical air temperatures, the UHI of three densely populated (urban) and one sparsely populated (suburban) area in Bangkok was 0.8 °C on average, with temperature differences reaching 6–7 °C during the summer months (March-May) [23]. Another research examined how LST and patterns of green space and impervious surfaces interacted in the urban areas of Bangkok, Jakarta, and Manila. They found that the mean LST had a negative correlation with green space areas and a positive correlation with impervious surface density. Furthermore, the mean LST of the study's urban regions' impervious surfaces was 3 °C higher than the green area's [24].

In the context of urban environments, which are extremely complex environmental systems with unique circumstances in every city, the spatiotemporal properties of surface biophysical features become important components of cityscapes and significant contributors to the SUHI effect [13, 25]. The main driving force behind the SUHI is one of the trickiest scientific problems. Numerous studies on the effects of LST on entrepreneurship have been carried out from a variety of angles [26]. Spectral markers for surface composition can be effectively chosen using four fundamental concepts and guidelines, as several research have shown: minimal redundancy, practical ubiquity, theoretical relevance, and simplicity of accessibility. Because spectral indices like the normalized difference built-up index (NDBI) [27], normalized difference moisture index (NDMI) [28], and modified normalized difference water body index (MNDWI) [29] are good at capturing surface biophysical features and have good correlations with LST, researchers have chosen to use them. Studies have shown that changes in land cover and land use significantly affect the SUHI intensity across a range of spatiotemporal conditions [30]. The study discovered that the geographical variability of LST patterns is a result of the integration of functions inside built-up areas brought about by fast urbanization [31]. The difficulties in acquiring precise data on urban morphology at fine scales, however, have prevented thorough investigations into the connections between the urban surface biophysics layer, landscape composition, and overheating in the developing tropics. Filling in the information gap about how urban features affect SUHIs in tropical cities is the goal of this study [24]. Specifically, it examines how surface biophysical characteristics and the thermal environment interact with urban land use planning, especially in tropical Asia, with a particular emphasis on a Thai city.

Thailand's capital, Bangkok (Krung Thep Maha Nakhon), has served as such for almost 200 years. The largest city in Thailand, it continues to be a major economic center. More than 10 million people are living in the region, making it a densely populated area [32]. Bangkok's population is constantly growing due to the city's economic opportunities mostly fuelled by rural-to-urban migration [33]. Urban sprawl, the growth of transportation networks, real estate markets, rising land values, and the

extension of cities into peripheral areas are all results of this quick increase in population, capital investment, factories, and workers [34]. The BMR was created by the growing urbanization of Bangkok and the five neighbouring provinces. An earlier investigation into the urbanization of BMR [35] emphasized that more than 70% of the developed areas formed from agricultural terrains throughout the 2000–2020 timeframe. World Bank population statistics (https://data.worldbank.org/country/thailand?view=chart) and the Statistical Report of Thailand (2020) (https://www.nso.go.th/public/e-book/Statistical-Yearbook/SYB-2020/6/) showed that the proportion of the country's population living in urban areas had increased significantly, rising from 22% in 1972 to 52% in 2020. Among the environmental problems brought on by the BMR's expansion include land subsidence, increased urban heat, and pollution of the air and water. According to the Thai Meteorological Department (TMD), Bangkok's maximum air temperatures have risen during the past 20 years. Previous studies on LST and SUHI in Bangkok found temperature risk areas mainly in Zones 1 and 2, with expansion driven by unplanned urbanization [36]. There are temperature differences between the urban and rural areas, as shown by multiple research projects, showing that Bangkok has a harsh urban climate that is associated with the phenomena of UHI. This focus is on the SUHI analysis with DLST and NLST, geospatial indices, and LULC alteration from 2015 to 2023. Urban warming mitigation solutions based on scientific understanding have received little attention from planners and stakeholders, despite several recent examinations into Bangkok's UHIs.

2. Study area

Bangkok's high population, tropical monsoon climate, and fast urbanization provide several environmental problems for Thailand's capital. With an average annual rainfall of roughly 1,500–2,000 mm, the city on the Chao Phraya River, receives ample rainfall, especially during the monsoon season, which runs from May to October. Bangkok frequently experiences temperatures between 25°C (77°F) to 35°C (95°F), with the hottest months happening immediately before the rainy season [37]. The heavy humidity makes the heat much worse, particularly in urban areas. Bangkok's dense concentration of roads, buildings, and other impermeable surfaces absorbs and retains heat throughout the day, making the city hotter than the nearby rural areas [38]. This phenomenon is known as the UHI effect and is one of the city's main environmental problems. Rapid urbanization, which decreases green spaces and increases the number of heat-retaining surfaces, exacerbates this effect. Greater energy use for cooling, poor air quality, and greater health risks, especially for vulnerable groups like children and the elderly, are all consequences of the UHI effect (Fig. 1).

The necessity of tackling these environmental issues has been acknowledged by the BMA and the Thai government. Numerous measures have been put in place to lessen the impact of the UHI effect, including the creation of more green areas, the encouragement of rooftop gardens, the installation of cool roofs, and urban shade programs [39]. The repair of existing parks and green spaces as well as the inclusion of green infrastructure in new construction are increasingly encouraged by urban planning regulations. In recognition of Bangkok's susceptibility to floods as a result of its low-lying terrain and heavy rainfall, the government has also made investments to strengthen flood management measures. This covers building retention ponds, canal restorations, and drainage systems. In response to the high traffic and pollution levels that contribute to the UHI impact, the government has improved bike lanes and pedestrian infrastructure while promoting public transit systems like the MRT Subway and BTS Skytrain [40]. Bangkok has integrated efforts to lower energy use and carbon emissions into its climate action plan, which emphasizes climate resilience and sustainability [41]. These government programs and urban planning techniques, despite the difficulties, are meant to improve Bangkok's environmental sustainability, increase the city's resistance to the effects of climate change, and improve the standard of living for its citizens. Bangkok aims to address its urban heat island impacts and other environmental challenges in the face of fast urban growth by continuing its efforts in flood control, climate action, and green infrastructure.

3. Materials and method

3.1. Data information

To obtain MODIS LST data in Google Earth Engine (GEE), use the MOD11A1 (Terra) and MYD11A1 (Aqua) datasets. With a scale of 0.02 (multiplied by 0.02), these offer daily Day (LST_Day_1km) and Night (LST_Night_1km) LST at a resolution of 1 km. To filter trustworthy pixels, Quality Control (QC_Day, QC_Night) flags are used. For research on climate change, land surface dynamics, and urban heat, the databases are perfect. They can be accessed with ee.ImageCollection('MODIS/061/MOD11A1'). In this work, both photos are used to calculate Bangkok's DLST and NLST between 2015 and 2023. From 2015

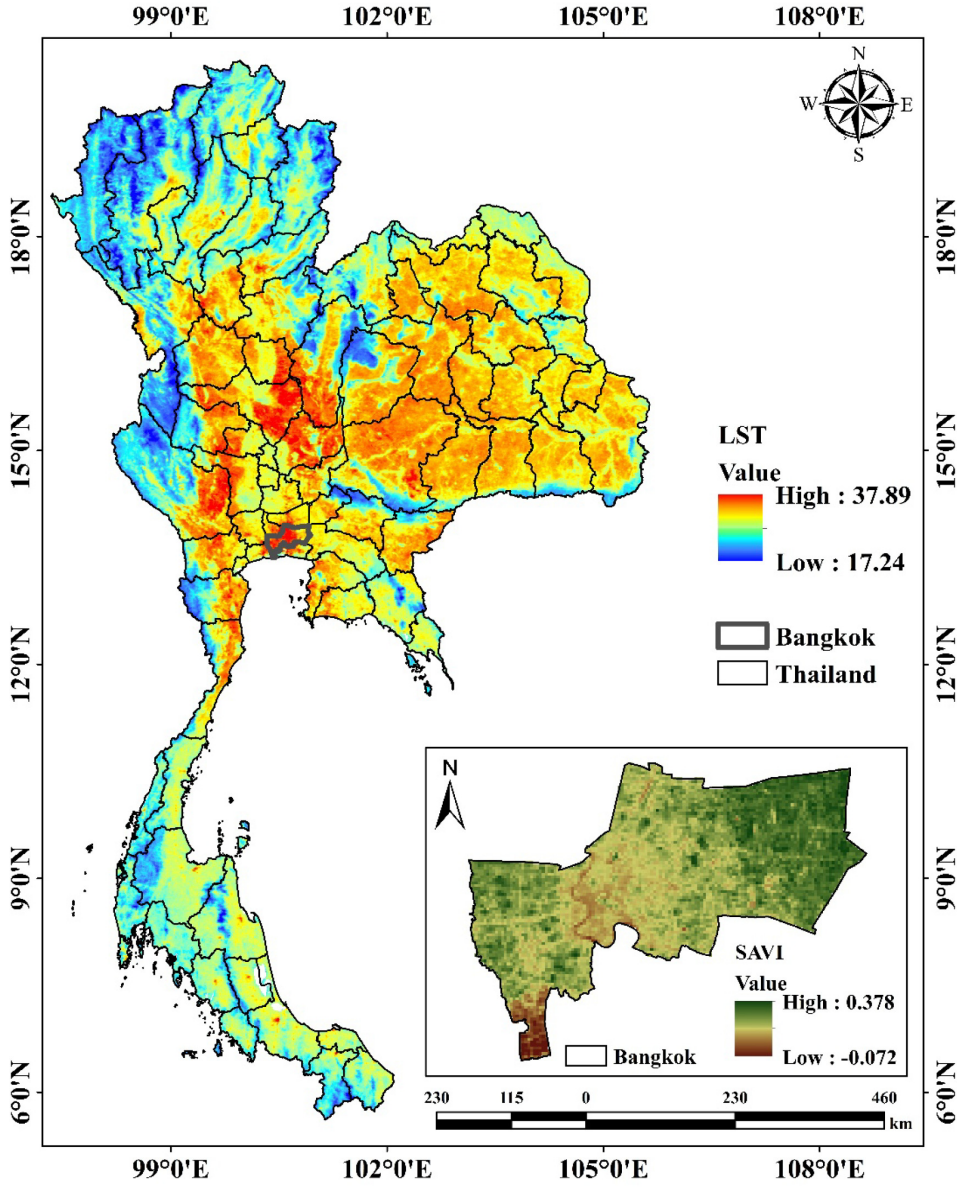

Fig. 1. Location map of Bangkok, Thailand.

to 2023, SAVI, NDBI, NDMI, and MNDWI can be calculated using Landsat 8 Surface Reflectance data (LANDSAT/LC08/C02/T1_L2) in Google Earth Engine. The following bands are used in the calculations: NIR (SR_B5), Red (SR_B4), SWIR1 (SR_B6), and Green (SR_B3). Indexes are obtained using altered formulas or normalized differences. Applying cloud masking and scaling (0.0000275) is necessary to achieve precise outcomes (Fig. 2).

3.2. LULC classification

To increase the precision and dependability of the final classification findings, pretreatment and postprocessing procedures are essential for LULC classification utilizing Landsat 8 data. Converting raw Landsat 8 data into a format that may be used is the first step in preprocessing. To enable precise comparison between various images and sensors, radiometric correction is usually used, which changes the Digital Numbers (DNs) to Top of Atmosphere (TOA) reflectance [20]. Geometric correction eliminates distortions brought on by sensor movement or the curvature of the Earth, ensuring that the image accurately corresponds with geographic coordinates [42]. Another crucial function of cloud masking is Removing clouds and their shadows, which might obstruct the classification of land cover. Additional

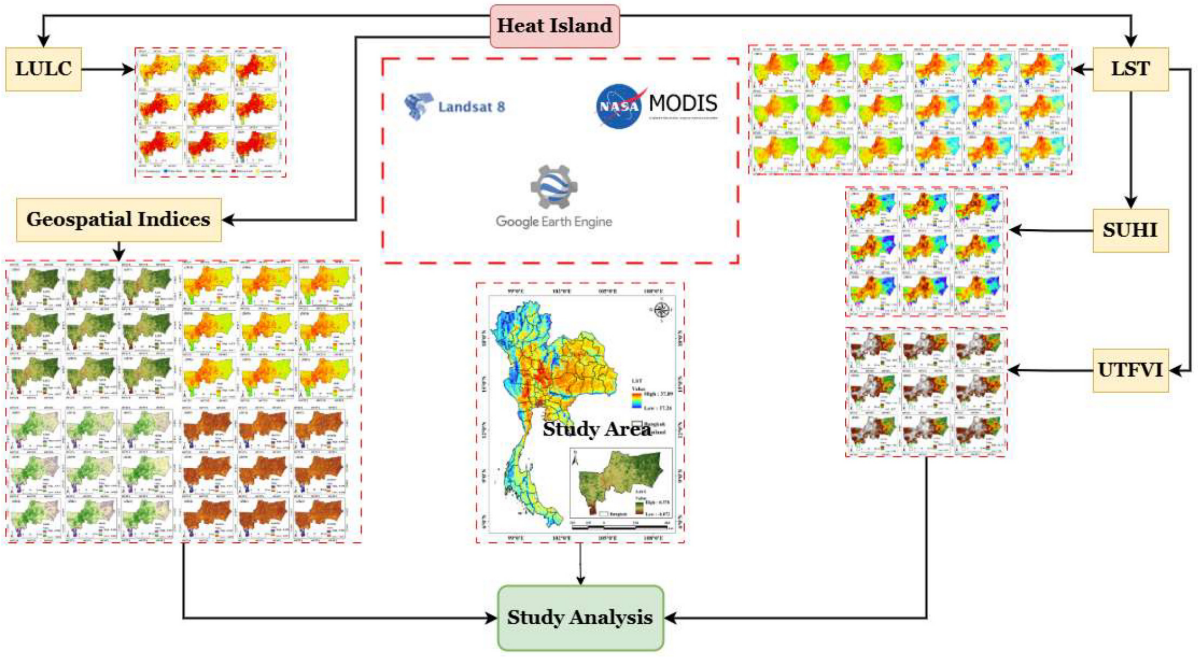

Fig. 2. Adopted methodology for SUHI study in Bangkok, Thailand from 2015 to 2023.

atmospheric adjustments can reduce the effects of atmospheric particles.

Supervised and unsupervised approaches might be used for the actual classification [43]. A classifier, such as Maximum Likelihood Classification (MLC) [44] or Support Vector Machine (SVM) [45], is used to assign land cover classes to the entire image based on training examples, chosen in supervised classification. Pixels are grouped into clusters using unsupervised classification methods such as K-means [46], and these clusters are subsequently manually labelled with the types of land cover they represent. The categorization outcomes are improved using post-processing procedures. A confusion matrix is used to compare the classification result to ground truth data to assess accuracy. To assess the success of the classifier, it is useful to compute measures such as overall accuracy, user accuracy, and producer accuracy. Noise, such as tiny, isolated pixels that don't accurately depict different types of land cover, can also be eliminated using post-classification filtering. Small gaps or the boundaries of the classification can be filled in by morphological processes like erosion or dilatation. Furthermore, the boundaries between different forms of land cover may be improved via edge refinement techniques.

Lastly, the GEE interface allows for the visualization of the classified map, which facilitates a rapid examination of the different types of land cover. The outcome can then be exported for additional analysis, either as a vector file or as a raster picture for GIS software, depending on the needs of the study. To sum up, the process of classifying LULC in GEE using Landsat 8 data combines preprocessing methods (such as radiometric correction and cloud masking), classification techniques (either supervised or unsupervised), and post-processing steps (such as filtering and accuracy assessment) [47]. For land cover mapping, monitoring, and decision-making, these procedures are necessary to guarantee that the final categorization is precise and significant.

3.3. Applied geospatial indices

To reduce the impact of soil background reflectance, particularly in regions with little vegetation cover, the SAVI vegetation index was created [48]. A variation of the NDVI, it is susceptible to the brightness of the soil, especially in areas with little vegetation. SAVI uses a soil adjustment factor (L) to monitor vegetation more precisely in different soil types. To draw attention to urban areas, the NDBI is a vegetation index that separates built-up surfaces including roads, buildings, and other infrastructure from non-built-up areas, such as vegetation and water bodies. Classifying urban land cover and tracking urban sprawl, particularly in satellite data, are two common uses for NDBI [49]. One vegetation indicator used to evaluate the moisture content of soil and vegetation is the NDMI. The NDMI is especially helpful for tracking drought conditions, vegetation stress, and moisture availability in the

landscape since it is sensitive to changes in moisture and water content, unlike the NDVI [50]. The Near-Infrared (NIR) and Short-Wave Infrared (SWIR) bands of satellite images are commonly used to calculate NDMI because they react differentially to soil and vegetation moisture levels. Since it can be challenging to distinguish between built-up and water areas using conventional vegetation indices like NDVI, the MNDWI is a vegetation index created to facilitate water body recognition. Particularly in metropolitan settings where other indices may have trouble detecting water bodies because of man-made surfaces, the MNDWI takes advantage of the green and SWIR bands, which are sensitive to water.

$$SAVI = \frac{(NIR - RED) \times (1 + L)}{(NIR + RED + L)} \tag{1}$$

$$NDBI = \frac{(SWIR - NIR)}{(SWIR + NIR)} \tag{2}$$

$$NDMI = \frac{(NIR - SWIR)}{(NIR + SWIR)} \tag{3}$$

$$\text{MNDWI} = \frac{(\text{Green} - SWIR)}{(\text{Green} + SWIR)} \tag{4}$$

The soil adjustment factor, L, varies from 0 (no soil influence) to 1 (highest soil effect), where NIR is the reflectance in the near-infrared band and RED is the reflectance in the red band. A typical value for L is 0.5. Reflectance in the Short-Wave Infrared (SWIR) band, usually Band 6 or Band 7 for Landsat imaging, is known as SWIR. NIR is near-infrared reflectance, usually found in Band 4 of Landsat imagery.

3.4. LST estimation

To estimate LST from MODIS data, the MODIS thermal infrared bands (Band 31 or 32) must be converted to LST [51, 52]. In particular, the MODIS LST products (MOD11A1 or MYD11A1), which are pre-processed and adjusted for atmospheric influences, can be used to estimate LST using MODIS data [53]. You can use the following procedures to determine LST directly from MODIS raw data:

Convert DN to TOA Radiance: For MODIS, the following formula is used to determine the TOA radiance, or (L_λ), from the raw DN:

$$L_\lambda = M_\lambda \times Q_{cal} + A_\lambda \tag{5}$$

Where: L_λ is the TOA radiance ($\text{W/m}^2 \cdot \text{sr} \cdot \mu\text{m}$), M_λ is the radiance multiplicative scaling factor (from metadata), A_λ is the radiance additive scaling factor (from metadata), Q_{cal} is the pixel value (DN).

TOA Radiance to Brightness Temperature Conversion (T_B): Next, use the following formula, which is derived from Planck's law, to convert the TOA radiance to brightness temperature:

$$T_B = \frac{K_2}{\ln(\frac{K_1}{L_\lambda} + 1)} \tag{6}$$

Where: T_B is the brightness temperature in Kelvin, K_1 and K_2 are the thermal calibration ↓constants (from the MODIS metadata).

Convert Brightness Temperature to LST: Utilizing an emissivity correction, brightness temperature, T_B is converted to LST. The following formula is frequently used:

$$LST = T_B \times \left(1 + \lambda \times T_B/\rho \times \ln(\epsilon)\right) \tag{7}$$

Where: T_B is the brightness temperature in Kelvin, λ is the wavelength of emitted radiance (11.03 μm for MODIS Band 31), ρ is a constant ($1.438 \times 10^4\ \mu\text{m} \cdot \text{K}$), ϵ is the emissivity can vary based on land cover type (urban, forest, water, etc.). In urban areas, ϵ typically ranges from 0.85 to 0.95. The final result, LST, is expressed in Kelvin, which can be converted to Celsius by subtracting 273.15.

3.5. Heat island measurement

The LST datasets and the notified formulation compute the heat island impacts. The SUHI study is required to calculate the Thailand heat island effect with seasonal change [13, 54]. To describe the impact of SUHI, the UTFVI is the primary instrument. Numerous factors affect LST that contribute to the SUHI and UTFVI phenomena [55, 56]. SUHI indicates the localized warming effect in urban areas as opposed to surrounding rural environments, while UTFVI is an index employing to classify the various levels of thermal stress within these urban areas. Severe thermal stress is indicated by higher UTFVI values and translates into increased health risks, greater energy consumption, and discomfort for residents living in urban environments. Heat waves, earth surface change, light intensity, and psychometrics are some variables.

$$\text{SUHI} = \left(\frac{\text{T}_\text{s} - \text{T}_\text{mean}}{\text{SD}}\right) \tag{8}$$

$$\text{UTFVI} = \left(\frac{\text{T}_\text{s} - \text{T}_\text{mean}}{\text{T}_\text{mean}}\right) \tag{9}$$

Where, T_s indicates LST in Kelvin, SD means standard deviation of LST, and T_mean representing mean values of LST.

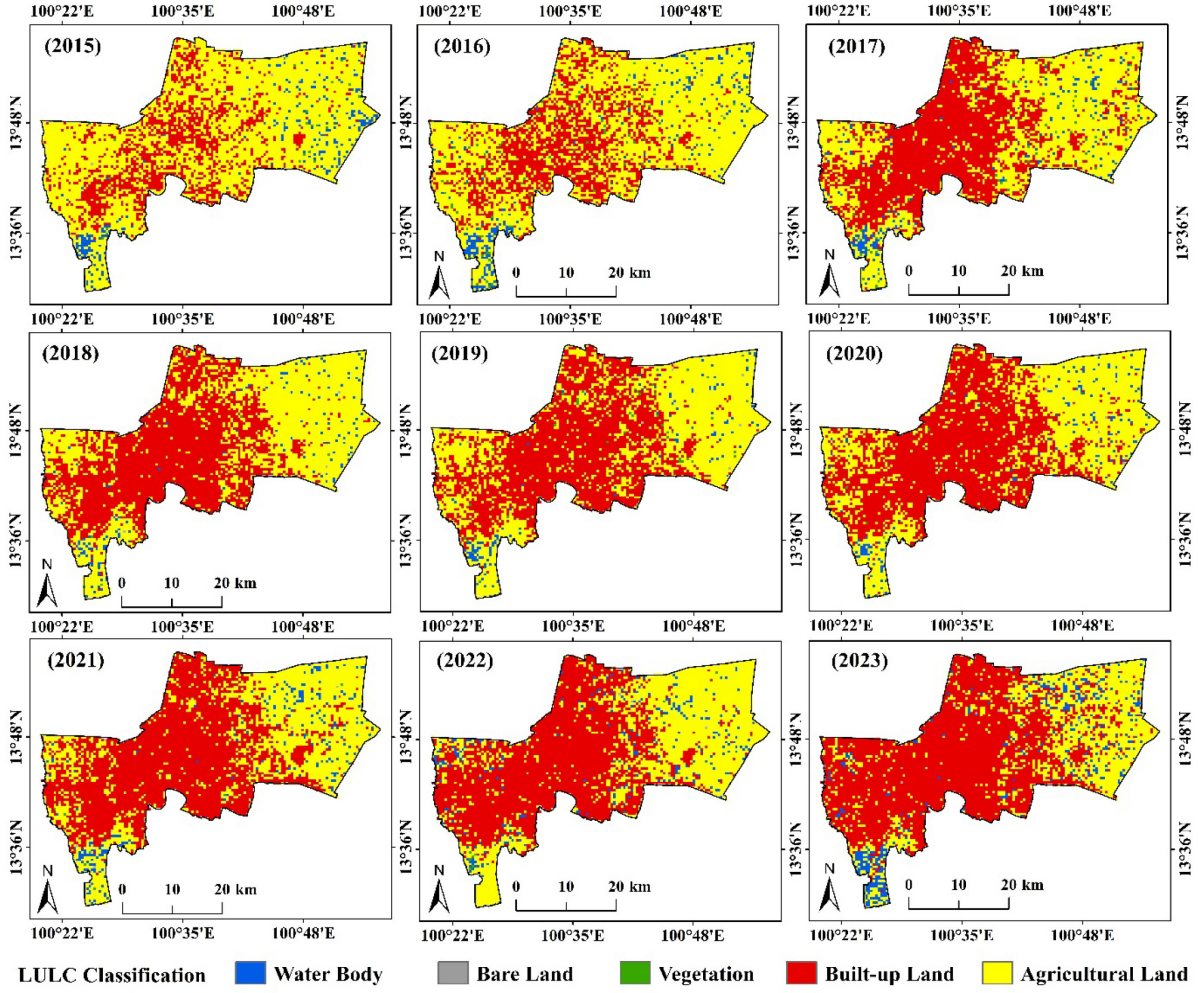

Fig. 3. LULC maps of Bangkok from 2015 to 2023.

4. Modeling results

4.1. LULC modeling

Rapid urbanization is responsible for the notable changes in the distribution of land types in Bangkok, as shown by the LULC maps from 2015 to 2023 (Fig. 3). Large portions of the city are now dominated by built-up territory, especially in the central and suburban sections, as a result of its significant expansion over time. Agricultural land, particularly in the outskirts, has been steadily declining as a result of this growth. Additionally, there is less bare ground and vegetation since many of these places have been turned into metropolitan centers to meet the demands of industry, commerce, and housing. Water bodies have remained relatively constant, with very slight variations in their spatial expanse. One possible explanation for this stability is the efforts to preserve natural water systems like canals and rivers. Nonetheless, the loss of agricultural land and the shrinking of green areas have serious environmental repercussions. Urban heat island effects are made worse by the dwindling flora, which also has a detrimental effect on biodiversity and carbon sequestration. Meanwhile, the risk of flooding rises when permeable surfaces are swapped out for impermeable ones, a serious issue in a city like Bangkok that experiences frequent flooding. The stresses of urban growth and the difficulties in striking a balance between development and environmental sustainability are highlighted by these developments. The increasing problems of urbanization and its effects on the environment and local populations call for the implementation of climate-resilient measures, sustainable urban design, and green infrastructure.

4.2. Geospatial indices measurement

After accounting for the impact of soil brightness, the SAVI maps of Bangkok from 2015 to 2023 offer

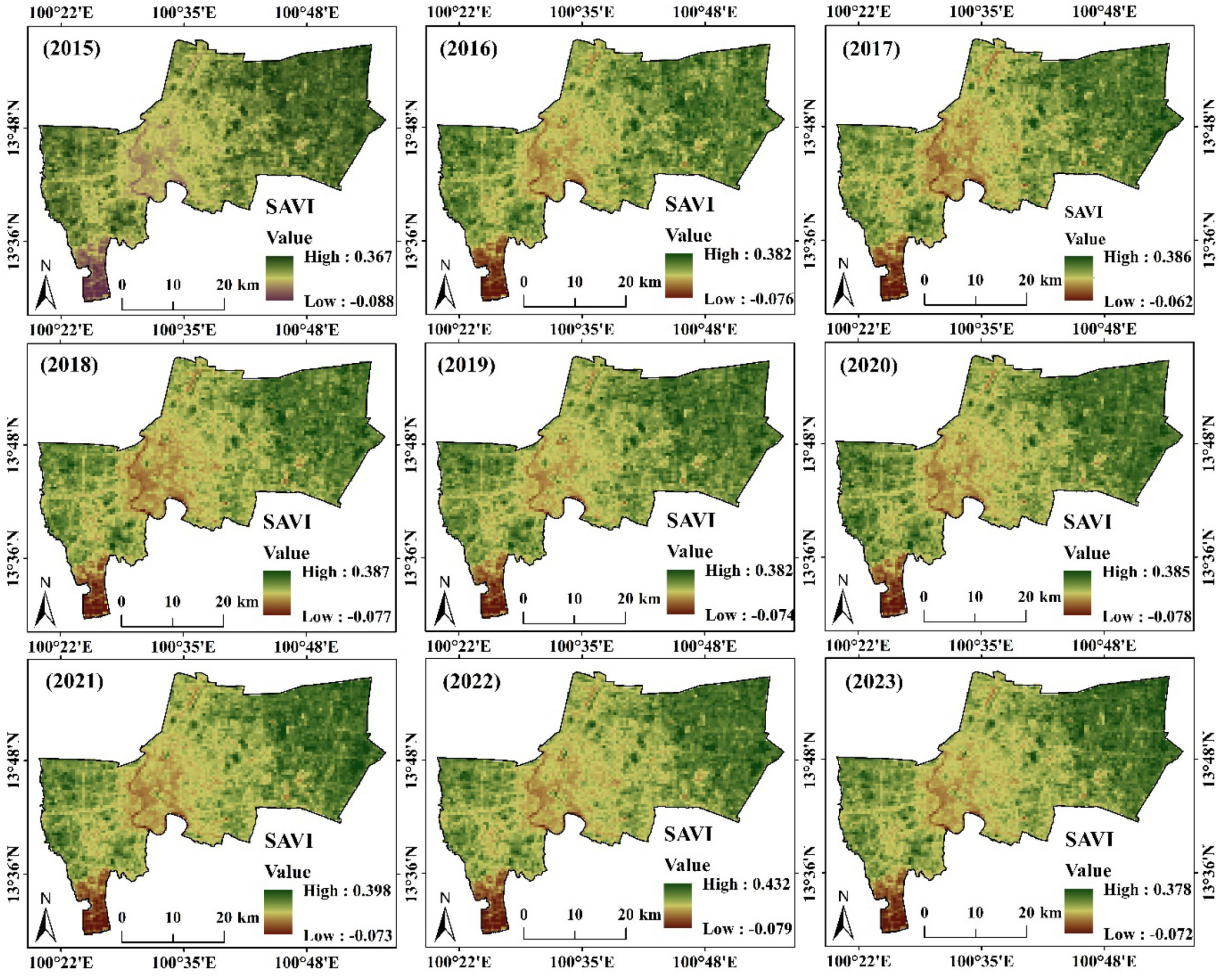

Fig. 4. SAVI maps of Bangkok from 2015 to 2023.

Table 1. Threshold values of the urban thermal field variance index (UTFVI) and ecological evaluation index [57].

Urban Thermal Field Variation Index	Urban Heat Island Phenomenon	Ecological Evaluation Index
<0	None	Excellent
0–0.005	Weak	Good
0.005–0.010	Middle	Normal
0.010–0.015	Strong	Bad
0.015–0.020	Stronger	Worse
>0.020	Strongest	Worst

information on the state of the local vegetation. Variations in vegetation density and health are reflected in the SAVI values, which vary from a low of roughly −0.088 to a high of 0.398 during the observed period. With greater values (over 0.36) localized in the periphery, where vegetation was denser, SAVI levels in 2015 were usually modest. Particularly in the city center and southern sections, urbanized or arid areas showed lower SAVI values (below −0.08). SAVI values varied throughout time as a result of shifting land uses, urbanization, and possible vegetation loss (Fig. 4). In 2021, the highest SAVI value of 0.398 was noted, signifying a peak in vegetation health and density that may have been caused by agricultural activity in some regions or urban greening initiatives. But in the years that followed, there was a minor drop, reaching a high of 0.378 in 2023. In a similar vein, the lowest scores, which fluctuated between −0.088 in 2015 and −0.072 in 2023, indicated areas that were consistently barren or heavily urbanized. Higher SAVI values were continuously seen in the northeastern and periphery regions between 2015 and 2023, indicating that these areas maintained superior vegetation cover (Table 2). On the other

Table 2. Maximum, minimum, and mean values of geospatial indices and LSTs (Day and Night).

Index	2015			2016			2017		
	Max	Min	Mean	Max	Min	Mean	Max	Min	Mean
5SAVI	0.367	–0.088	0.1395	0.382	–0.076	0.153	0.386	–0.062	0.162
NDBI	0.057	–0.479	–0.211	0.062	–0.465	–0.2015	0.065	–0.0429	0.01105
NDMI	0.479	–0.057	0.211	0.466	–0.062	0.202	0.429	–0.065	0.182
MNDWI	0.649	–0.301	0.174	0.596	–0.298	0.149	0.598	–0.287	0.1555
DLST	36.77	27.18	31.975	36.81	27.38	32.095	36.76	25.62	31.19
NLST	27.38	23.78	25.58	26.91	24.01	25.46	27.91	22.82	25.365
Index	2018			2019			2020		
	Max	Min	Mean	Max	Min	Mean	Max	Min	Mean
SAVI	0.387	–0.077	0.155	0.382	–0.074	0.154	0.385	–0.078	0.1535
NDBI	0.078	–0.477	–0.1995	0.083	–0.466	–0.1915	0.067	–0.473	–0.203
NDMI	0.477	–0.078	0.1995	0.466	–0.083	0.1915	0.445	–0.022	0.2115
MNDWI	0.641	–0.272	0.1845	0.654	–0.296	0.179	0.631	–0.306	0.1625
DLST	36.93	27.56	32.245	38.39	26.66	32.525	37.61	26.89	32.25
NLST	27.05	23.15	25.1	27.09	23.96	25.525	27.28	23.52	25.4
Index	2021			2022			2023		
	Max	Min	Mean	Max	Min	Mean	Max	Min	Mean
SAVI	0.398	–0.073	0.1625	0.432	–0.079	0.1765	0.378	–0.072	0.153
NDBI	0.081	–0.451	–0.185	0.106	–0.46	–0.177	0.077	–0.435	–0.179
NDMI	0.4	–0.066	0.167	0.404	–0.062	0.171	0.417	–0.048	0.1845
MNDWI	0.642	–0.29	0.176	0.628	–0.297	0.1655	0.594	–0.317	0.1385
DLST	38.14	25.85	31.995	37.35	26.01	31.68	37.72	25.62	31.67
NLST	26.72	22.64	24.68	27.36	22.87	25.115	27.08	23.74	25.41

hand, Bangkok's central and southern regions consistently displayed lower SAVI values, which is consistent with the city's continued urbanization and shrinkage of green areas as shown by LULC research.

NDBI values from 2015 to 2023 are shown in the figure, emphasizing the growth of built-up areas over time. Non-built-up areas, such as vegetation or water bodies, are indicated by lower or negative NDBI values, whereas built-up or urbanized areas are indicated by larger positive values. During the nine years, the maximum NDBI values have increased significantly, especially between 2015 (0.057) and 2021 (0.081), indicating steady urban growth. Although the lowest values fluctuate somewhat, from −0.479 in 2015 to −0.435 in 2023, the overall trend shows a decline in non-built-up regions (Fig. 5). Particularly in the center and southern regions, urban areas shown on the map as red zones have progressively grown, perhaps encroaching on green or natural areas. Among previous years, 2018 had the greatest maximum NDBI score (0.078), indicative of an increase in development or building activities. The slightly lower maximum value (0.077) in 2023, on the other hand, can point to a plateau in urban growth or changing patterns of urbanization. The 2021 and 2023 minimum values, which are −0.451 and −0.435, respectively, indicate a progressive decline of vegetated or unbuilt-up areas over time. The necessity for housing, infrastructure, and commercial development frequently results in a loss of natural land cover, and this trend is consistent with the rapid urbanization trends frequently seen in places like Bangkok. The changes that have been noticed highlight the continuous change in land use in the region, which may be influenced by demographic expansion, economic expansion, and development initiatives. These trends could have an impact on environmental sustainability, necessitating balanced urban development to reduce the effects of urban heat islands and conserve undeveloped areas.

As vegetation moisture levels decreased over time, the maximum NDMI values gradually decreased from 2015 to 2023, from 0.479 in 2015 to 0.417 in 2023. This loss raises the possibility of environmental stress brought on by deforestation, fast urbanization, or climate variables that impact the health of vegetation. The lowest NDMI values, which indicate greater urban coverage and less non-urban vegetation zones, also exhibit significant variances, ranging from −0.078 in 2018 to −0.048 in 2023 (Fig. 6). The continuous influence of urban development on natural land cover is demonstrated by the steady growth of arid zones, which are indicated by low NDMI values (Table 2). The maximum NDMI readings in 2018 briefly increased to 0.477, perhaps as a result of better water availability for plants or favourable meteorological circumstances. The readings began to decline once more in 2021 when the highest NDMI fell precipitously to 0.400, but this recovery was not maintained in the following years. Some mitigation

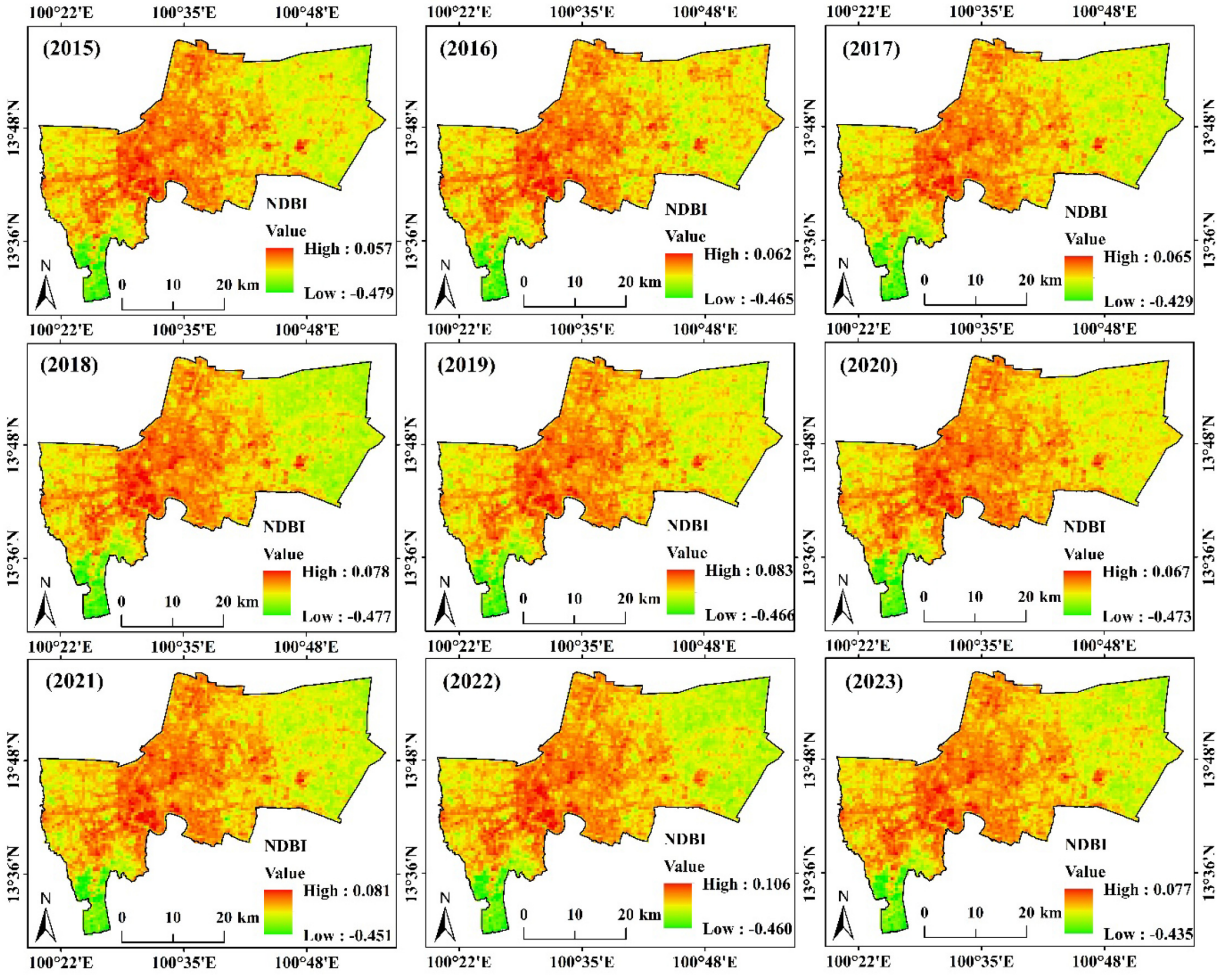

Fig. 5. NDBI maps of Bangkok from 2015 to 2023.

of extreme dryness is suggested by a minor improvement in minimum NDMI values by 2023 (-0.048), which could be achieved by local conservation initiatives or adjustments to land management techniques. The patterns that have been seen are consistent with the fast urbanization occurring in and around Bangkok, where urban infrastructure is replacing green spaces and agricultural regions, lowering the overall moisture content of the vegetation. Additionally, the annual variations in NDMI values are probably caused by seasonal rainfall variability influenced by monsoon patterns. The study emphasizes the necessity of efficient water management and sustainable urban design to mitigate the negative environmental effects of continued urbanization and maintain the region's vegetation health.

Probably in an area close to Bangkok, the image shows changes in the amount of water and non-water surfaces over time, illustrating MNDWI values from 2015 to 2023. MNDWI values are a range of negative to positive, with positive values denoting water bodies like rivers, lakes, or wetlands and negative values representing non-water surfaces like urban or vegetated regions. During 2015–2023, the maximum MNDWI values dropped from 0.649 to 0.594, indicating a decline in the intensity or coverage of water bodies. Similarly, minimum values changed from −0.301 in 2015 to −0.317 in 2023, indicating that land-use changes or urbanization may have increased the number of non-water surfaces (Fig. 7). Some years, like 2017 and 2023, saw notable fluctuations, with maximum values sharply declining, suggesting that water bodies were under stress from the environment or infrastructure. Rapid urbanization in the Bangkok area, where built-up regions have supplanted natural water bodies, and seasonal or climatic factors like rainfall unpredictability may be to blame for these patterns. These changes may also be influenced by land reclamation initiatives or other water management techniques like canal alterations. The trends that have been noticed highlight the necessity of water conservation initiatives and sustainable

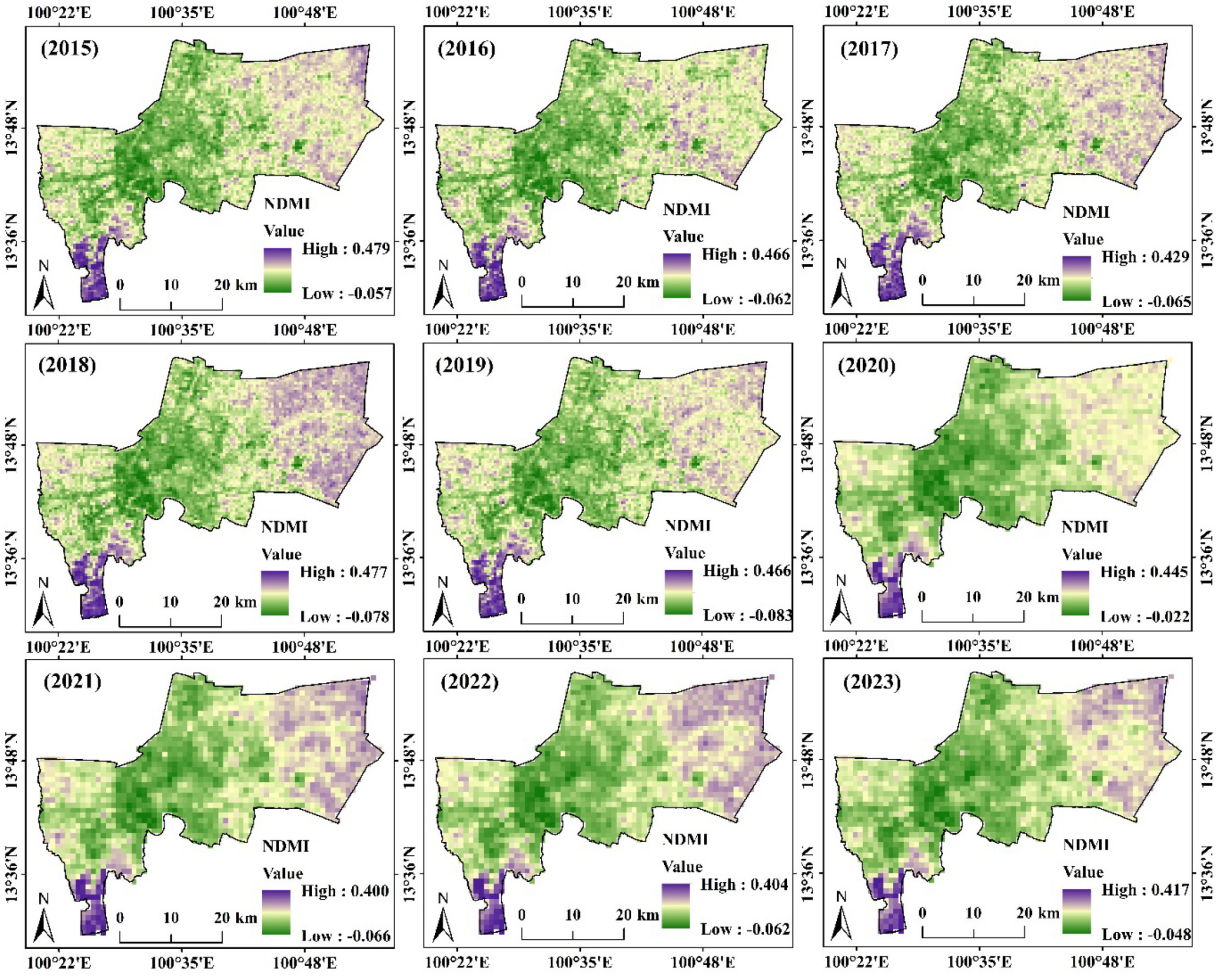

Fig. 6. NDMI maps of Bangkok from 2015 to 2023.

urban design to handle the continuous changes in the hydrological and land-use dynamics of the area.

4.3. LST analysis

The maximum DLST shows a consistent upward trend, peaking at 38.14°C in 2021 after rising from 36.77°C in 2015, then slightly declining to 37.22°C in 2023. With no discernible pattern, the minimum DLST varies between 25.62°C and 27.56°C, potentially as a result of shifting vegetation and land use (Fig. 8). In terms of geography, the central and northern regions continuously show increasing DLST values, indicating an urban heat island effect, while the southern parts continue to be cooler, most likely as a result of vegetation or water bodies. Between 2019 and 2021, the maximum DLST increased significantly, suggesting that warming was accelerated over this time, maybe due to urbanization or climate extremes. From 9.49°C in 2015 to 11.60°C in 2021 (Table 3), the thermal range between the highest and minimum DLST increased with time, suggesting that surface temperature is becoming more heterogeneous. Although they are still higher than in previous years, maximum temperatures show little stability after 2021 [58]. These patterns highlight how human activity and climate change affect local temperature dynamics, highlighting the significance of environmental preservation and urban planning in preventing more warming.

The maximum NLST varies slightly over time, from 26.91°C in 2016 to 27.48°C in 2015, reaching a peak of 27.28°C in 2020 before levelling off at 27.08°C in 2023 (Fig. 9). The measured timeframe suggests that evening thermal conditions are rather steady, as evidenced by the slight range in the maximum nighttime temperatures. However, the minimum NLST has greater variability, fluctuating between 22.64°C in 2021 and 24.01°C in 2016, with sporadic cooling trends probably impacted by regional environmental factors such as atmospheric dynamics or vegetation cover. Lower temperatures (green zones) are found

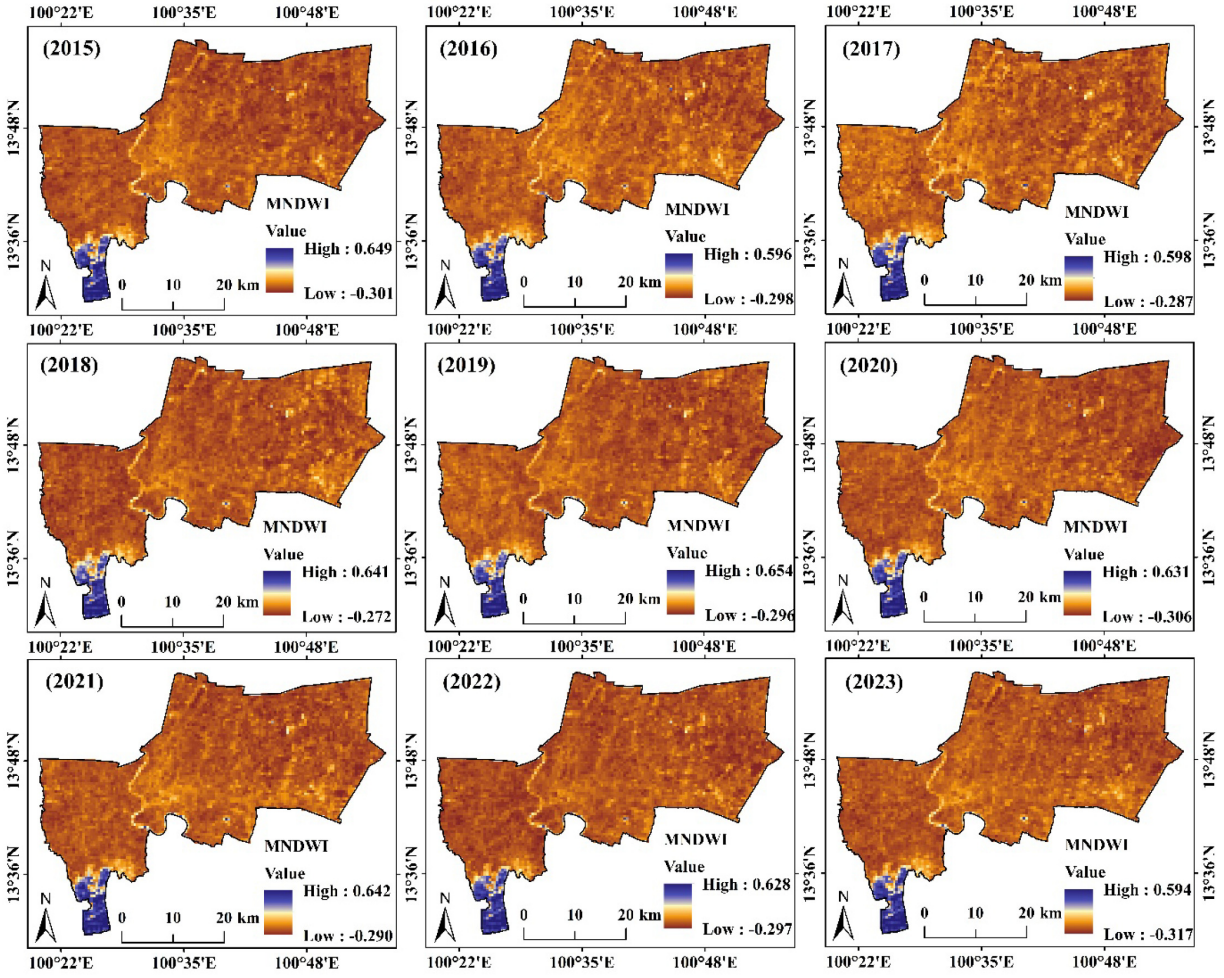

Fig. 7. MNDWI maps of Bangkok from 2015 to 2023.

in the southern and periphery, while higher temperatures (red zones) are concentrated in the center and northern regions [32]. Due to decreased nighttime cooling and heat storage in impermeable surfaces, these patterns point to urban heat retention in the core zones. Cooler zones are those that have vegetation or bodies of water, which help to provide efficient cooling at night. The difference between the maximum and minimum NLST, or thermal contrast, varies throughout time from roughly 3°C to 4.5°C, reaching its highest in 2018 (27.05°C to 23.13°C). This suggests a rise in thermal variability in the area, which may be caused by changes in land use or urbanization. Following 2020, a minor downward trend in the thermal range is noted, indicating that nocturnal temperatures may have stabilized as a result of either natural or man-made causes. Between 2019 and 2020, both the maximum and minimum NLST had the biggest rises in nighttime temperatures, which may be the result of extreme weather occurrences or transient climatic shifts. There may be a levelling-off effect in the observed region, as the temperature trends after 2021 stay comparatively consistent.

4.4. SUHI measurement

SUHI intensity in Bangkok from 2015 to 2023 is shown in the presented image, emphasizing spatiotemporal variability. Higher numbers indicate stronger urban heat effects in the assessed SUHI intensity. The following is a thorough analysis: There is a general increase in the maximum SUHI intensity from 1.112 (2015) to 1.162 (2021), and then a minor decrease to 1.157 (2023). Urban heat effects have been getting stronger over time, as evidenced by this upward trend. This is probably because of growing urbanization, rising anthropogenic heat emissions, and declining plant cover. The geographical variations in land cover or nighttime cooling effectiveness may be the cause of the slight fluctuations in the lowest

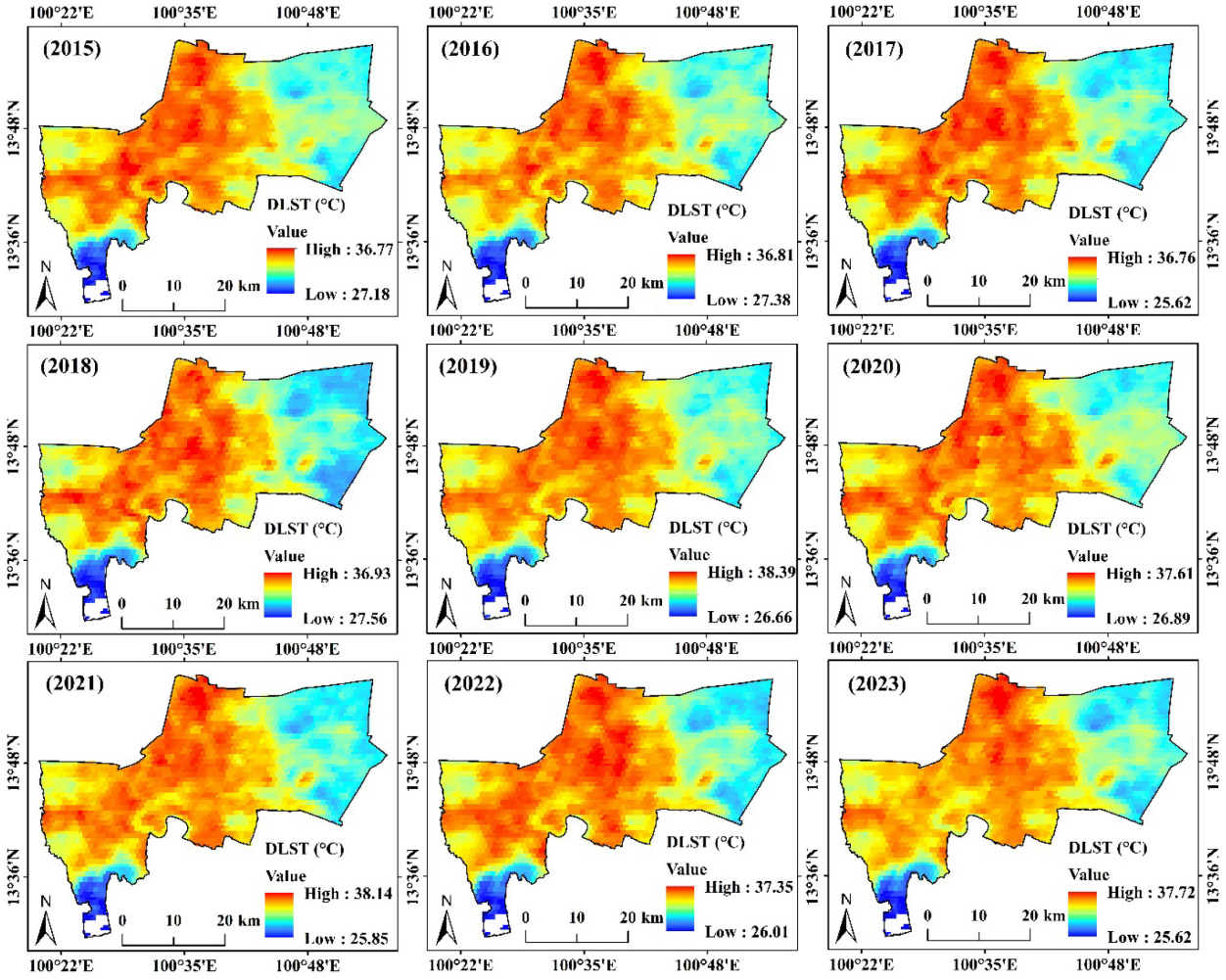

Fig. 8. Daytime LST maps of Bangkok from 2015 to 2023.

Table 3. Maximum, minimum, and mean values of SUHI and UTFVI.

Indices	2015			2016			2017		
	Max	Min	Mean	Max	Min	Mean	Max	Min	Mean
SUHI	1.119	0.777	0.948	1.112	0.779	0.9455	1.153	0.751	0.952
UTFVI	11.06	7.68	9.37	11.6	8.12	9.86	11.9	7.75	9.825
Indices	2018			2019			2020		
	Max	Min	Mean	Max	Min	Mean	Max	Min	Mean
SUHI	1.123	0.813	0.968	1.119	0.746	0.9325	1.097	0.757	0.927
UTFVI	11.42	8.27	9.845	10.99	7.32	9.155	11.33	7.82	9.575
Indices	2015			2016			2017		
	Max	Min	Mean	Max	Min	Mean	Max	Min	Mean
SUHI	1.162	0.756	0.959	1.169	0.785	0.977	1.157	0.755	0.956
UTFVI	12.01	7.82	9.915	12.39	8.33	10.36	12.19	7.96	10.075

SUHI intensity, which ranges from 0.746 (2018) to 0.813 (2018). Darker orange to red zones, which indicate the highest SUHI intensities, are consistently seen in the core urban regions (Fig. 10). Due to their sparse greenery, impermeable surfaces, and dense urban infrastructure, these locations probably retain heat and have a lower capability for cooling. The vegetative and peripheral zones, on the other hand, exhibit lower SUHI values (blue and green), highlighting the natural land cover's moderating effect on surface temperature regulation. With the maximum value increasing slightly from 1.112 to 1.123, the

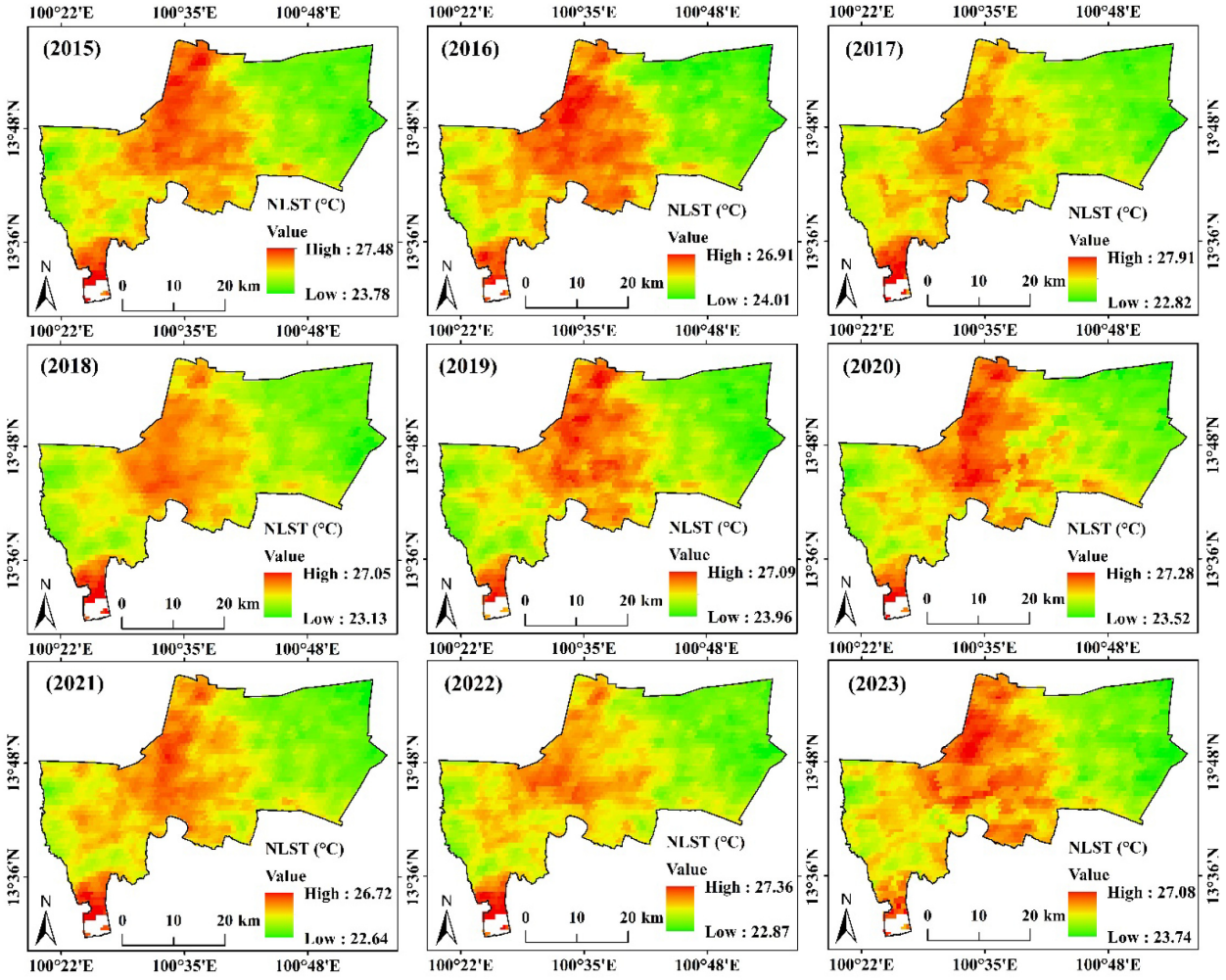

Fig. 9. Night-time LST maps of Bangkok from 2015 to 2023.

SUHI intensity suggests a mild increase from 2015 to 2018 (Table 3). A greater increase in SUHI intensity is noted between 2018 and 2021, which corresponds with fast urbanization and potential reductions in green cover. Since 2021, the highest SUHI values have stabilized somewhat, which may indicate that the urban heat effect's severity has plateaued or that mitigation efforts, including urban greening projects, have begun to offset the heat accumulation.

The shifting levels of heat stress in Bangkok are depicted on the UTFVI maps from 2015 to 2023. The UTFVI values range from 11.06 in 2015 to 12.19 in 2023, indicating an increasing trend in thermal intensity over time, according to the maps (Fig. 11). This suggests that the UHI impact is gradually but noticeably getting stronger, especially in crowded and built-up areas. The central and southern regions consistently exhibit higher UTFVI values, often exceeding 11.0 in later years, reflecting the heat-retaining capacity of urbanized zones with impervious surfaces like asphalt and concrete. Because of the vegetation and open spaces that help moderate temperatures, the northeastern regions, on the other hand, continue to be somewhat colder, with UTFVI values falling below 8.0 for several years. With the highest values circling 11.0 and the lowest around 7.32, UTFVI readings stayed reasonable between 2015 and 2018 (Table 3). Nonetheless, there has been a discernible increase in high-heat zones since 2019, with peak UTFVI values continuously exceeding 11.0 and rising to 12.19 by 2023. This trend emphasizes the increasing heat stress in cities, probably caused by growing urbanization, a decline in green space, and rising temperatures associated with climate change. The results highlight how urgently sustainable urban planning solutions like adding more vegetation, installing green roofs, and using water features in urban planning are needed. By taking these steps, Bangkok's citizens can live better, increase urban resilience, and lessen the city's increasing thermal stress.

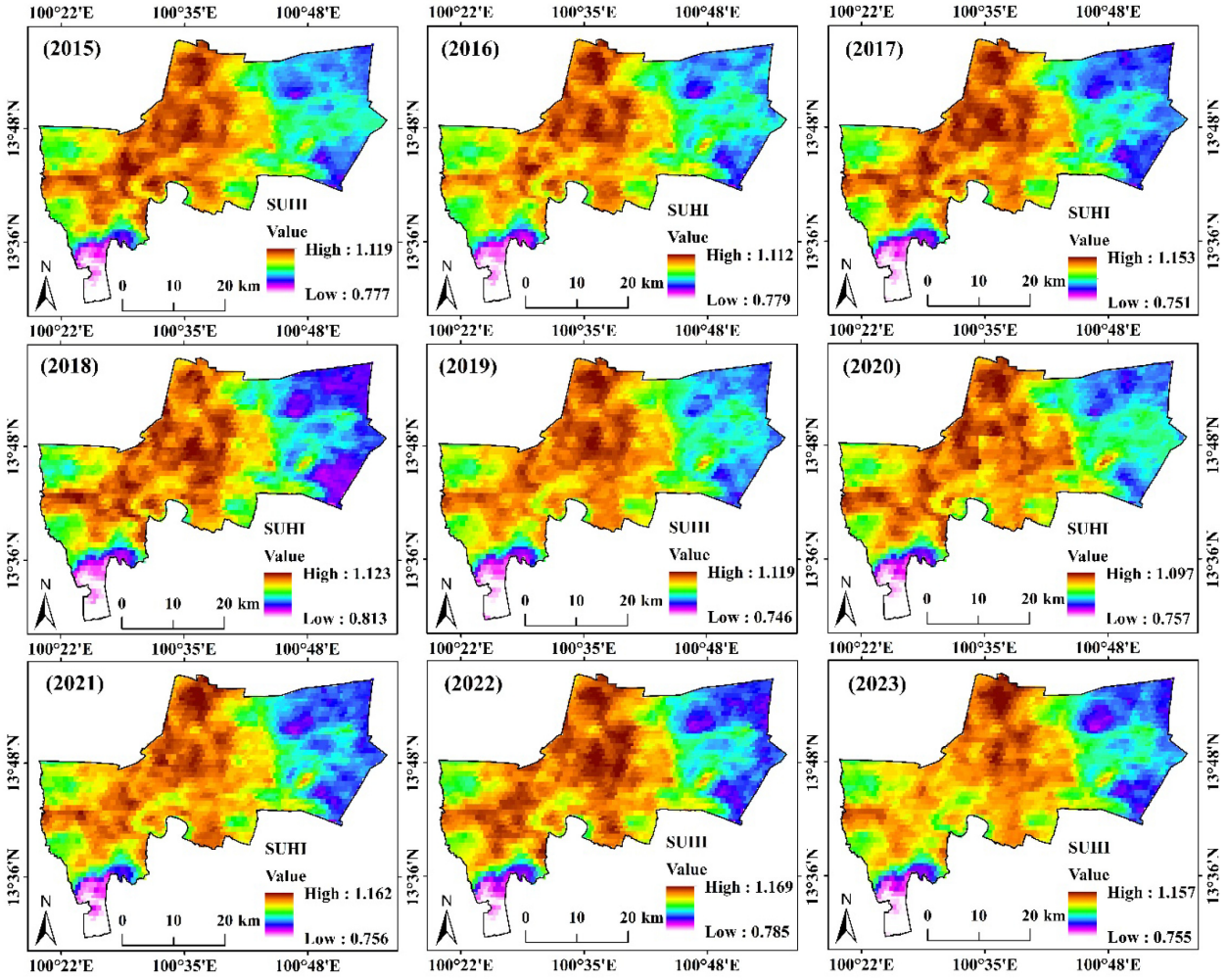

Fig. 10. SUHI maps of Bangkok from 2015 to 2023.

5. Discussion

A minor increase in thermal heterogeneity throughout the region is also reflected in the temperature range between the maximum and least SUHI readings [59]. This expanding range suggests that some outlying places may cool or keep constant temperatures as a result of improved environmental management, even as the metropolitan centers continue to heat up. Notably, southern areas near water bodies, such as the Chao Phraya River, consistently display lower SUHI intensities, reinforcing the cooling effect of water and vegetation [36]. In contrast, the northern regions that are heavily urbanized and industrialized exhibit consistent high-intensity values. The information emphasizes how urgently specific urban design measures are needed to lessen the consequences of SUHI, such as expanding green roofs, planting trees, and encouraging permeable surfaces. The stability of SUHI intensity beyond 2021 indicates that current efforts may be helpful, but more action and monitoring are needed to manage future temperature increases and enhance urban resilience. In urbanized areas, the general trend shows a slow deterioration in vegetation density and health, highlighting the necessity of strategies to preserve and increase vegetation to lessen the negative environmental effects of urbanization, such as lower air quality and urban heat island effects [60].

The spatial and temporal patterns of urban heat intensity throughout Bangkok are depicted in the UTFVI maps from 2015 to 2023. The charts show a distinct trend of rising heat stress, especially in the southern and central regions likely the most populated. As a result of continued urbanization and land-use changes, the regions with the highest thermal intensity have grown over time. Warmer regions are shown in red, while cooler regions are shown in green, creating a clear visual representation

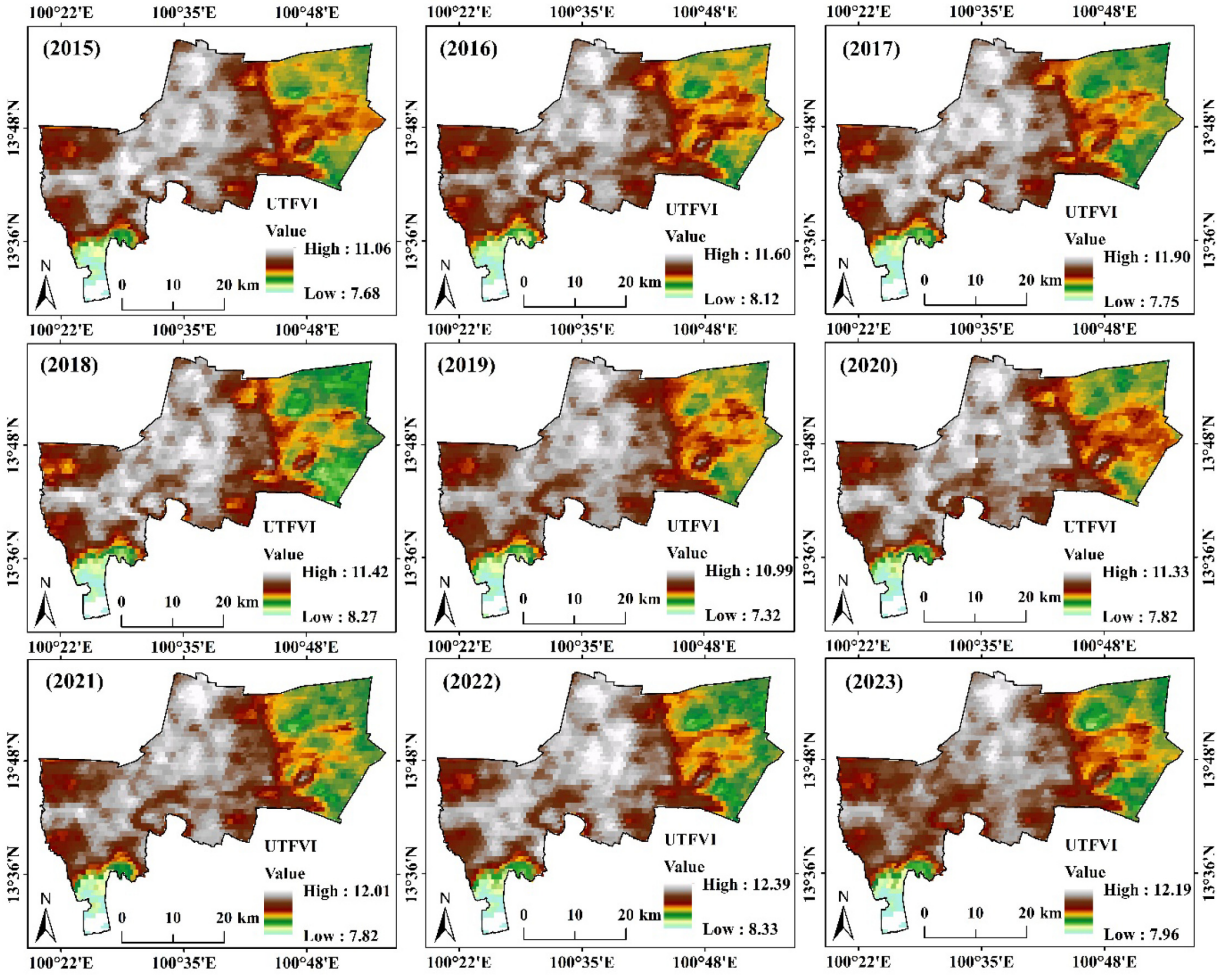

Fig. 11. UTFVI maps of Bangkok from 2015 to 2023.

of the temperature variation. Because there is more vegetation, open space, or water bodies to prevent heat buildup, the northeastern areas of the city always seem cooler. On the other hand, heat is persistent and getting worse in highly populated places, which is a sign of the urban heat island effect, which occurs when heat is trapped by impermeable surfaces like asphalt and concrete. Rising ambient temperatures brought on by climate change, decreased vegetation cover, and greater urbanization are probably the main causes of the thermal intensity's evolution throughout time [16]. Urban areas' ability to retain heat is increased by these changes, which reduces the thermal comfort of the environment. The significance of implementing sustainable urban planning techniques, such as maintaining green areas, encouraging energy-efficient building designs, and incorporating natural cooling components like urban trees and water bodies, is highlighted by these developments. In a rapidly urbanizing city like Bangkok, addressing these thermal concerns is crucial to enhancing urban liability and resilience.

Built-up land predominates in Bangkok's center districts, including Phra Nakhon, Bang Rak, and Pathum Wan, where the UHI effect is particularly noticeable. Because of their impermeable surfaces, dense urban infrastructure, and sparser vegetation, these regions routinely have higher UTFVI values, which indicate greater surface temperatures. These zones were subject to ongoing thermal stress from 2015 to 2023; UTFVI values were higher than 11.0 in 2021 and 2023, especially during increased urban activity. Conversely, the northeastern districts of Min Buri, Nong Chok, and Lat Krabang continue to have lower UTFVI values, indicating superior thermal comfort brought about by a mix of sparse urbanization, agricultural areas, and water bodies. These areas are vital defences against the city's worsening heat island effect. There are noticeable geographical changes in the vegetation health as measured by SAVI. Because of their agricultural areas and green belts, Bangkok's northeastern

and eastern districts often have higher SAVI values (over 0.36). In 2021, Nong Chok and Lat Krabang, for example, recorded SAVI values close to 0.39, indicating healthy vegetative cover. Conversely, SAVI scores below 0.10, which indicate scarce or nonexistent vegetation, are seen in central urbanized zones including Khlong Toei, Ratchathewi, and Sathon. Due to the substantial loss of vegetation in these densely populated, high-rise building-dominated areas, there is less capability for urban cooling and carbon sequestration.

Previous studies highlighted how high-rise structures and open areas enrich metropolitan landscapes by promoting better air circulation through roads [16, 24, 61]. Furthermore, academic discussions have emphasized the significance of including green spaces and designing buildings in an efficient manner [34, 37]. Therefore, it is necessary to take into account additional aspects that impact environmental difficulties while analysing metropolitan districts or localized contexts. The proportions of building height to road width and the arrangement of tall buildings are examples of these variables. Furthermore, the integration of green spaces takes the form of various characteristics and designs specific to each location, depending on the surrounding circumstances, financial limitations, and intended use as determined by landscape architects and urban planners [62]. Previous research in the BMR relied on LST data to explain this phenomenon, but by basing its analysis on air temperature data, this work closed the methodological gap in urban climatology. The potential of near-surface temperature analysis to produce an urban climate map that supports UHI mitigation is highlighted by this. Furthermore, it showed a more noticeable spatiotemporal variation than LST data [63]. Enhancing BMR thermal data and honing urban thermal studies through the use of a variety of climate data would require substantial work.

Changes in land usage are closely related to variations in temperature throughout Bangkok. Higher thermal variance is seen in central areas like Bang Sue and Huai Khwang, where the loss of green spaces and growing urban density have caused temperatures to rise sharply [64]. In the western districts, such as Bang Khae and Taling Chan, the conversion of agricultural land to urban infrastructure has also led to an increase in thermal stress over time [65]. The cooling influence of water bodies and mangrove forests, on the other hand, results in mild thermal conditions in regions along the Chao Phraya River, such as Samut Prakan and Bang Khun Thian. However, these regions are becoming more and more strained due to their expanding urbanization, which results in gradual warming. Built-up areas have significantly expanded in Bangkok, with urban development cantered in the central and western districts. Over time, Lat Phrao, Bang Kapi, and Don Mueang have changed, with bare terrain and agriculture being turned into residential and commercial areas [66]. This quick development increases surface temperatures, decreases vegetation health, and intensifies the effects of UHI. Urbanization has been slower in the northeastern districts, such as Sai Mai and Bang Bo, which still feature a mix of agricultural and vegetated regions. To lessen Bangkok's urban sprawl's negative environmental effects, these areas are essential.

The rise in urban temperatures across Bangkok is closely linked to changes in land use, particularly urban expansion and the reduction of green spaces. Central districts like Bang Sue and Huai Khwang experience higher temperatures due to rapid urbanization, while western areas such as Bang Khae and Taling Chan face increased thermal stress from agricultural land conversion. Water bodies and mangrove forests along the Chao Phraya River help regulate temperatures, but ongoing urbanization threatens their cooling effects. Preserving green spaces, implementing sustainable urban planning, and promoting reflective materials are crucial in mitigating the urban heat island effect and ensuring a more resilient city environment.

6. Limitations and future research direction

The poor geographic resolution (1 km) of MODIS data, which ignores fine-scale urban fluctuations, and the fact that it measures surface temperature rather than air temperature are two of its drawbacks for Bangkok's UHI investigations [52]. Accuracy is decreased by air interference, cloud cover, and urban heterogeneity; further difficulties arise from significant preprocessing and ground validation. For reliable analysis, MODIS must be complemented with ground-based or higher-resolution data. Landsat data is better suited to capturing fine-scale urban fluctuations in Bangkok's UHI investigations since it has a higher spatial resolution (30 m) than MODIS [67]. Nevertheless, the monitoring of dynamic temperature changes is limited by its lower temporal resolution (16-day revisit). There are still issues with cloud cover, atmospheric interference, and the emphasis on surface temperature rather than air temperature. Although merging Landsat with other data sources can yield a more thorough UHI study, extensive preprocessing and validation are necessary. The results obtained from this study will have great social relevance in urban planning, public health, and sustainable development matters. Hence, lessons learned

from this study could enable policymakers to apply focused interventions to remedy various high-risk heat-stress zones in and around Bangkok and other cities through the expansion of green areas and heat-resilient building materials, ensuring full comfort for the population.

The interdependence of vegetation health, UHI, and thermal variation highlights the negative environmental effects of Bangkok's fast urbanization. Because of the severe heat stress and vegetation loss experienced by central districts, immediate solutions such as rooftop gardens, urban greening, and sustainable zoning laws are required. Despite being ecological buffers at the moment, peripheral districts may lose their environmental integrity due to growing urban pressures. It is crucial to combine development with environmental sustainability by keeping vegetation in the northeastern and eastern zones, protecting mangroves along the river, and incorporating green infrastructure into urban planning. To address these issues and guarantee Bangkok's resilience to urbanization and climate change, a multifaceted strategy is needed. These NLST trends highlight how important nocturnal urban heat retention is and how it interacts with climate variability. They also emphasize the necessity of urban cooling techniques to lessen the consequences of nighttime warming, such as introducing heat-reflective materials or expanding vegetative cover. Recent NLST stability indicates that, if applied, interventions may already be having some effect; however, this has to be confirmed by additional research and ongoing monitoring.

7. Conclusion

In summary, Bangkok's UHI, vegetation health, thermal fluctuation, and urban development from 2015 to 2023 are examined, highlighting the increasing environmental problems brought on by the city's rapid urbanization. The center districts have severe vegetation loss and increased UHI impacts due to their densely populated areas, which exacerbates thermal stress and lowers overall liability. Expanding urban infrastructure is putting more and more strain on the peripheral regions, especially in the northeast and east, which are crucial biological zones with healthier vegetation and less thermal volatility. Temperature variations are directly related to changes in land cover and use, as urbanization has gradually displaced agricultural and vegetated regions, especially in the west and south. Despite their continued existence, the cooling benefits of the Chao Phraya River and the nearby mangrove forests are becoming more and more threatened by encroaching urbanization. Adopting sustainable urban design techniques, such as incorporating green infrastructure, preserving vegetation-rich regions, and putting heat-mitigation techniques like rooftop gardens, urban parks, and permeable surfaces into practice, is crucial to overcoming these obstacles. Additionally, sustaining the city's natural balance depends on focused efforts to protect mangrove regions along the river and ecological zones in the northeastern districts. Bangkok's capacity to strike a balance between urban growth and environmental sustainability will determine how resilient it is in the future. An urban environment that is healthier, more liveable, and climate resilient will require proactive steps to reduce thermal stress, improve vegetation health, and control urban sprawl.

Ethical approval

None.

Conflict of interest

No conflicts of interest exist to declare.

Funding statement

None.

Author contribution

None.

Data availability

None.

References

1. S. Lolli, Y.-C. Chen, S.-H. Wang, and G. Vivone, "Impact of meteorological conditions and air pollution on COVID-19 pandemic transmission in Italy," *Sci. Rep.*, vol. 10, p. 16213, 2020. doi:10.1038/s41598-020-73197-8.
2. Z. Zhao, X. Yang, H. Yan, Y. Huang, G. Zhang, T. Lin, H. Ye, and S. Bonafoni, "Remote sensing downscaling building energy consumption carbon emissions by machine learning," 2021. doi:10.3390/rs13214346.
3. N. Gorai, J. Bandyopadhyay, B. Halder, M. F. Ahmed, A. H. Molla, and T. M. T. Lei, "Spatio-temporal variation in landforms and surface urban heat island in riverine megacity," *Sustainability*, vol. 16, p. 3383, 2024.
4. B. M. Hashim, A. Al Maliki, M. A. Sultan, S. Shahid, and Z. M. Yaseen, "Effect of land use land cover changes on land surface temperature during 1984–2020: A case study

of Baghdad city using landsat image," *Nat. Hazards*, 2022. doi:10.1007/s11069-022-05224-y.
5. D. Sánchez González, "Peligrosidad y exposición a los ciclones tropicales En ciudades del golfo de México: El caso de tampico," *Rev. Geogr. Norte Gd.*, pp. 151–170, 2011.
6. K. Z. Tun, M. Pramanik, R. Chakrabortty, K. Chowdhury, B. Halder, C. B. Pande, A. Mukhopadhyay, and M. Zhran, "Mainstreaming nature-based solutions for climate adaptation in southeast asia: A systematic review," *Earth Syst. Environ.*, pp. 1–19, 2024.
7. B. Halder, "Remote sensing-based optimal electric vehicle charging station identification in Kolkata urban agglomeration," *Transp. Res. Part D Transp. Environ.*, vol. 139, p. 104580, 2025.
8. P. V. de Azevedo, P. T. da Costa Bezerra, M. Ramos Leitão M. V. B. de, and C. A. C. dos Santos, "Thermal comfort level assessment in urban area of petrolina-PE county, Brazil X1 - avaliação do nível de conforto térmico na área urbana do município de petrolina-PE," Brasil. *Rev. Bras. Meteorol.*, vol. 32, pp. 555–563, 2017. doi:10.1590/0102-7786324004.
9. N. A. S. Kasniza Jumari, A. N. Ahmed, Y. F. Huang, J. L. Ng, C. H. Koo, K. L. Chong, M. Sherif, and A. Elshafie, "Analysis of urban heat islands with landsat satellite images and GIS in Kuala Lumpur metropolitan city," *Heliyon*, vol. 9, pp. e18424–e18424, 2023. doi:10.1016/j.heliyon.2023.e18424.
10. R. Chakrabortty, M. Pramanik, M. M. Hasan, B. Halder, C. B. Pande, K. N. Moharir, and M. Zhran, "Mitigating urban heat islands in the global south: Data-driven approach for effective cooling strategies," *Earth Syst. Environ.*, pp. 1–28, 2024.
11. B. Halder, J. Bandyopadhyay, and N. Ghosh, "Remote sensing-based seasonal surface urban heat island analysis in the mining and industrial environment," *Environ. Sci. Pollut. Res.*, pp. 1–34, 2024.
12. G. Ulpiani, "On the linkage between urban heat island and urban pollution island: Three-Decade literature review towards a conceptual framework," *Sci. Total Environ.*, vol. 751, p. 141727, 2021. doi:10.1016/j.scitotenv.2020.141727.
13. T. Chakraborty, A. Hsu, D. Manya, and G. Sheriff, "A spatially explicit surface urban heat island database for the united states: Characterization, uncertainties, and possible applications," *ISPRS J. Photogramm. Remote Sens.*, vol. 168, pp. 74–88, 2020. doi:10.1016/j.isprsjprs.2020.07.021.
14. B. M. Hashim, A. N. A. Alnaemi, M. A. Sultan, E. A. Alraheem, S. A. Abduljabbar, B. Halder, S. Shahid, and Z. M. Yaseen, "Impact of climate change on land use and relationship with land surface temperature: Representative case study in iraq," *Acta Geophys.*, pp. 1–19, 2025.
15. B. Halder, A. Karimi, P. Mohammad, J. Bandyopadhyay, R. D. Brown, and Z. M. Yaseen, "Investigating the relationship between land alteration and the urban heat island of seville city using multi-temporal landsat data," *Theor. Appl. Climatol.*, 2022. doi:10.1007/s00704-022-04180-8.
16. P. Iamtrakul, A. Padon, and J. Klaylee, "Analysis of urban sprawl and growth pattern using geospatial technologies in Megacity, Bangkok, Thailand," In *Proc. of the International Conference on Geoinformatics and Data Analysis*, Springer, 2022, pp. 109–123.
17. T. Hutton and R. Paddison, "Cities and economic change: Restructuring and dislocation in the global metropolis," 2014.
18. J. Yang, Y. Wang, C. Xiu, X. Xiao, J. Xia, and C. Jin, "Optimizing local climate zones to mitigate urban heat island effect in human settlements," *J. Clean. Prod.*, 2020. doi:10.1016/j.jclepro.2020.123767.
19. J. V. Henderson, "Cities and development," *J. Reg. Sci.*, vol. 50, pp. 515–540, 2010.
20. M. D. Negassa, D. T. Mallie, and D. O. Gemeda, "Forest cover change detection using geographic information systems and remote sensing techniques: A spatio-temporal study on komto protected forest priority area," East Wollega Zone, Ethiopia. *Environ. Syst. Res.*, vol. 9, 2020. doi:10.1186/s40068-020-0163-z.
21. B. Halder, P. Chatterjee, B. Rana, J. Bandyopadhyay, C. B. Pande, K. O. Ahmed, I. Elkhrachy, and N. Radwan, "Delineating the climate change impacts on urban environment along with heat stress in the Indian tropical city," *Phys. Chem. Earth, Parts A/B/C*, vol. 136, p. 103745, 2024.
22. N. Thanvisitthpon, A. Nakburee, D. Khamchiangta, and V. Saguansap, "Climate change-induced urban heat island trend projection and land surface temperature: A case study of Thailand's Bangkok metropolitan," *Urban Clim.*, vol. 49, p. 101484, 2023.
23. D. Khamchiangta and S. Dhakal, "Physical and non-physical factors driving urban heat island: Case of Bangkok metropolitan administration, Thailand," *J. Environ. Manage.*, vol. 248, p. 109285, 2019.
24. R. C. Estoque, Y. Murayama, and S. W. Myint, "Effects of landscape composition and pattern on land surface temperature: An urban heat island study in the megacities of Southeast Asia," *Sci. Total Environ.*, vol. 577, pp. 349–359, 2017. doi:10.1016/j.scitotenv.2016.10.195.
25. O. R. García-Cueto, E. Jáuregui-Ostos, D. Toudert, and A. Tejeda-Martinez, "Detection of the urban heat island in mexicali, B. C., México and its relationship with land use," *Atmósfera*, vol. 20, pp. 111–131, 2007.
26. P. Mohammad, A. Goswami, and S. Bonafoni, "The impact of the land cover dynamics on surface urban heat island variations in semi-arid cities: A case study in Ahmedabad city, India, using multi-sensor/source data," *Sensors*, vol. 19, p. 3701, 2019. doi:10.3390/s19173701.
27. M. Fontanelli, M. Pirchio, B. Halder, J. Bandyopadhyay, A. Ali Al-Hilali, A. M. Ahmed, M. W. Falah, S. Ali Abed, K. T. Falih, and K. Mohamed Khedher, *et al.*, "Assessment of urban green space dynamics influencing the surface urban heat stress using advanced geospatial techniques," 2022. doi:10.3390/agronomy12092129.
28. S. Rahman and V. Mesev, "Change vector analysis, tasseled cap, and NDVI-NDMI for measuring land use/cover changes caused by a sudden short-term severe drought: 2011 texas event," *Remote Sens.*, vol. 11, p. 2217, 2019.
29. H. Xu, "Modification of normalised difference water index (NDWI) to enhance open water features in remotely sensed imagery," *Int. J. Remote Sens.*, vol. 27, pp. 3025–3033, 2006.
30. A. Siddiqui, G. Kushwaha, B. Nikam, S. K. Srivastav, A. Shelar, and P. Kumar, "Analysing the day/night seasonal and annual changes and trends in land surface temperature and surface urban heat island intensity (SUHII) for Indian cities," *Sustain. Cities Soc.*, vol. 75, p. 103374, 2021.
31. I. Castro-Mendoza, J. R. Valdez-Lazalde, G. Donovan, T. Martínez-Trinidad, F. O. Plascencia-Escalante, and W. Vázquez-Morales, "Does Land-Use affect the temperature distribution across the city of Tuxtla gutiérrez, Chiapas, México? X1 - ¿El Uso de Suelo Afecta La Distribución de temperatura En La Ciudad de Tuxtla Gutiérrez, Chiapas, México?," *Investig. geográficas*, p. e60394–e60394, 2022. doi:10.14350/rig.60394.
32. T. Ngamsiriudom and T. Tanaka, "Making an urban environmental climate map of the Bangkok metropolitan region,

Thailand: Analysis of air temperature, wind distributions, and spatial environmental factors," *World Dev. Sustain.*, vol. 3, p. 100105, 2023.
33. T. G. McGee and I. M. Robinson, *The Mega-Urban Regions of Southeast Asia*, UBC Press, 1995, vol. 1, ISBN 077480548X.
34. Y. Shao *Mapping and Modeling the Urban Landscape in Bangkok, Thailand: Physical-Spectral-Spatial Relations of Population-Environmental Interactions*, The University of North Carolina at Chapel Hill, 2007, ISBN 0549126678.
35. A. Padon, P. Iamtrakul, R. Jintamethasawat, and J. Klaylee, "Spatial multicriteria evaluation for future urban growth in Bangkok metropolitan region: BMR," In *Proc. of the 2022 International Conference and Utility Exhibition on Energy, Environment and Climate Change (ICUE)*, IEEE, 2022, pp. 1–8.
36. L. Pan, L. Lu, P. Fu, V. Nitivattananon, H. Guo, and Q. Li, "Understanding spatiotemporal evolution of the surface urban heat island in the Bangkok metropolitan region from 2000 to 2020 using enhanced land surface temperature," *Geomatics, Nat. Hazards Risk*, 2023. doi:10.1080/19475705.2023.2174904.
37. D. O'Kane, "The ecological and social effects of gentrification and urbanisation in Thailand's lower Chao Phraya Delta," 2022.
38. P. Srisuwan and K. Shoichi, "Field investigation on indoor thermal environment of a high-rise condominium in hot-humid climate of bangkok, thailand," *Procedia Eng.*, vol. 180, pp. 1754–1762, 2017.
39. X. Yao, K. Yu, X. Zeng, Y. Lin, B. Ye, X. Shen, and J. Liu, "How can urban parks be planned to mitigate urban heat island effect in "furnace cities"? An Accumulation Perspective," *J. Clean. Prod.*, 2022. doi:10.1016/j.jclepro.2021.129852.
40. Z. Xie, "Intention of BTS skytrain passengers to use QR ticket for metro mass transit system in bangkok," 2023.
41. C. Chaiya, "Empowering Climate Resilience: A People-Centered Exploration of Thailand's Greenhouse Gas Emissions Trading and Sustainable Environmental Development through Climate Risk Management in Community Forests," *Heliyon*, 2025.
42. P. P. Gogoi, V. Vinoj, D. Swain, G. Roberts, J. Dash, and S. Tripathy, "Land use and land cover change effect on surface temperature over eastern India," *Sci. Rep.*, vol. 9, p. 8859, 2019. doi:10.1038/s41598-019-45213-z.
43. W. A. Bagwan and R. S. S Gavali, "Dam-Triggered land use land cover change detection and comparison (transition matrix method) of urmodi river watershed of Maharashtra, India: A remote sensing and GIS approach," *Geol. Ecol. Landscapes*, 2021. doi:10.1080/24749508.2021.1952762.
44. S. Reis, "Analyzing land use/land cover changes using remote sensing and GIS in rize, North-East Turkey," *Sensors (Basel)*, vol. 8, pp. 6188–6202, 2008. doi:10.3390/s8106188.
45. M. Hemmat Esfe, A. Tatar, M. R. H. Ahangar, and H. Rostamian, "A comparison of performance of several artificial intelligence methods for predicting the dynamic viscosity of TiO_2/SAE 50 nano-lubricant," *Phys. E Low-dimensional Syst. Nanostructures*, vol. 96, pp. 85–93, 2018. doi:10.1016/J.PHYSE.2017.08.019.
46. K. Jas and G. R. Dodagoudar, "Explainable machine learning model for liquefaction potential assessment of soils using XGBoost-sHAP," *Soil Dyn. Earthq. Eng.*, vol. 165, p. 107662, 2023. doi:10.1016/j.soildyn.2022.107662.
47. O. K. Gee and M. L. R. Sarker, "Monitoring the effects of land use/landcover changes on urban heat island," In Proc. of the Earth Resources and Environmental Remote Sensing/GIS Applications IV, SPIE, 2013, vol. 8893, pp. 20–27.
48. V. M. Rodríguez-Moreno and S. H. Bullock, "Comparación Espacial y Temporal de Índices de La Vegetación Para Verdor y Humedad y Aplicación Para Estimar LAI En El Desierto Sonorense X1 - comparison of vegetation indexes in the sonoran desert incorporating soil and moisture indicators and applicatio," *Rev. Mex. ciencias agrícolas*, vol. 4, pp. 611–623, 2013.
49. A. Varshney, "Improved NDBI differencing algorithm for built-up regions change detection from remote-sensing data: An automated approach," *Remote Sens. Lett.*, vol. 4, pp. 504–512, 2013.
50. A. P. Guilherme, A.B. S. Mota, D. S. Mota, N. G. Machado, and M. S. Biudes, "Uso De Índice De Vegetação Para Caracterizar a Mudança No Uso Do Solo Em COARI-AM X1 - Use of vegetation index to characterize the land use change in coari - AM," *Soc. Nat.*, vol. 28, pp. 301–310, 2016. doi:10.1590/1982-451320160209.
51. S.C. Lima, M. Neto, J. M. de, J. P. Lima, F.C. Lima, and L. M. F Saboya, "Response of semi-arid vegetation to agricultural drought determined by indices derived from MODIS satellite X1 - resposta Da Vegetação Semiárida à Seca Agrícola determinada Por Índices derivados Do Satélite MODIS," *Rev. Bras. Eng. Agrícola e Ambient.*, vol. 27, pp. 632–642, 2023. doi:10.1590/1807-1929/agriambi.v27n8p632-642.
52. M. F. Nejad and A. Zoratipour, "Assessment of LST and NDMI indices using MODIS and landsat images in karun riparian forest," *J. For. Sci.*, vol. 65, pp. 27–32, 2019.
53. Z. Wan, "A generalized split-window algorithm for retrieving land-surface temperature from space," *IEEE Trans. Geosci. Remote Sens.*, vol. 34, pp. 892–905, 1996. doi:10.1109/36.508406.
54. J. A. Sobrino and I. Irakulis, "A methodology for comparing the surface urban heat island in selected urban agglomerations around the world from sentinel-3 SLSTR data," *Remote Sens.*, vol. 12, pp. 1–31, 2020. doi:10.3390/RS12122052.
55. F. A. Abir, S. Ahmmed, S. H. Sarker, and A. U. Fahim, "Thermal and ecological assessment based on land surface temperature and quantifying multivariate controlling factors in Bogura, Bangladesh," *Heliyon*, vol. 7, pp. e08012–e08012, 2021. doi:10.1016/j.heliyon.2021.e08012.
56. N. Kikon, P. Singh, S. K. Singh, and A. Vyas, "Assessment of urban heat islands (UHI) of noida city, India using multi-temporal satellite data," *Sustain. Cities Soc.*, 2016.
57. L. Liu and Y. Zhang, "Urban heat island analysis using the landsat TM data and ASTER data: A case study in Hong Kong," *Remote Sens.*, 2011. doi:10.3390/rs3071535.
58. E. P. Agency, "Climate change indicators: Weather and climate," 2016.
59. D. Zhou, J. Xiao, S. Bonafoni, C. Berger, K. Deilami, Y. Zhou, S. Frolking, R. Yao, Z. Qiao, and J. Sobrino, "Satellite remote sensing of surface urban heat islands: Progress, challenges, and perspectives," *Remote Sens.*, vol. 11, p. 48, 2018. doi:10.3390/rs11010048.
60. C. V. F. de Souza, R. H. Oliveira Rangel, and M. Cataldi, "Avaliação Numérica Da Influência Da Urbanização No Regime de Convecção e Nos Padrões de Precipitação Da Região Metropolitana de São Paulo X1 - Numerical evaluation of the influence of urbanization in the convection and precipitation patterns in the metro," *Rev. Bras. Meteorol.*, vol. 32, pp. 495–508, 2017. doi:10.1590/0102-7786324001.
61. K. Irvine, F. Likitswat, A. Sahavacharin, A. Suwanarit, T. Lertwarapornpong, and D. Chitwatkulsiri, "The agrihood design: Valuation of ecosystem services for NbS visions in peri-urban housing estate development, Bangkok, Thailand," *J. Archit. Res. Stud.*, vol. 21, pp. 115–140, 2023. doi:10.56261/jars.v21.257520.

62. C. Liping, S. Yujun, and S. Saeed, “Monitoring and predicting land use and land cover changes using remote sensing and GIS techniques-A case study of a hilly area, Jiangle, China,” *PLoS One*, vol. 13, pp. e0200493–e0200493, 2018. doi:10.1371/journal.pone.0200493.
63. B. Halder, J. Bandyopadhyay, and P. Banik, “Monitoring the effect of urban development on urban heat island based on remote sensing and geo-spatial approach in Kolkata and adjacent areas, India,” *Sustain. Cities Soc.*, vol. 74, p. 103186, 2021. doi:10.1016/J.SCS.2021.103186.
64. S. Bunnarong and P. Upala, “Analysis of pedestrian crash zones in Bangkok: A case study of primary and secondary school,” *J. East. Asia Soc. Transp. Stud.*, vol. 12, pp. 1096–1113, 2017.
65. P. Varnakovida and H. Y. K. Ko, “Urban expansion and urban heat island effects on Bangkok metropolitan area in the context of eastern economic corridor,” *Urban Clim.*, vol. 52, p. 101712, 2023.
66. J. M. Gibson, “The application of transit development zones in Bangkok: The laksi case study,” 2011.
67. J. I. Souto O. de, and J. C. P. Cohen, “Spatiotemporal variability of urban heat island: Influence of urbanization on seasonal pattern of land surface temperature in the metropolitan region of Belém, Brazil,” *urbe. Rev. Bras. Gestão Urbana*, p. 13, 2021. doi:10.1590/2175-3369.013.e20200260.